Development of direct-current, atmospheric-pressure, glow discharges generated in contact with flowing electrolyte solutions for elemental analysis by optical emission spectrometry

Piotr Jamroz, Krzysztof Greda, Pawel Pohl

Direct-current, atmospheric-pressure, glow discharge (dc-APGD) generated in contact with flowing sample solutions is a new, very promising excitation source for analytical optical emission spectrometry, due to its low maintenance requirements and its analytical performance. Since analyzed solutions act as liquid cathodes, this discharge system is useful for the direct determination of elements dissolved in solutions without having to produce their aerosols by pneumatic nebulization.

The review presents different systems and designs of dc-APGD generated with the liquid cathode applied to spectrochemical analysis in the past 20 years. We discuss the effect of experimental conditions on analytical response and performance of the discharge. We include analytical figures of merit obtained with different discharge systems and their application to the analysis of environmental and biological samples containing various trace elements.

Keywords: Analytical figure of merit; Analytical performance; Direct-current, atmospheric-pressure, glow discharge (dc-APGD); Electrolyte solution; Elemental analysis; Liquid cathode; Mass spectrometry (MS); Optical emission spectrometry (OES); Spectrochemical analysis; Trace analysis

Piotr Jamroz, Krzysztof Greda, Pawel Pohl*
Analytical Chemistry Division, Faculty of Chemistry, Wroclaw University of Technology, Wybrzeze Stanislawa Wyspianskiego 27, Wroclaw 50–370, Poland

*Corresponding author.
Tel.: +48 71 320 3445;
Fax: +48 71 320 2494;
E-mail: pawel.pohl@pwr.wroc.pl

1. Introduction

The need for compact portable instruments that can be operated in the field for on-line analyses is one of the most important motivations for developing and miniaturizing analytical measurement systems and radiation sources used in atomic and mass spectrometry [1–7]. Indeed, small sizes and weights of various microplasmas and microdischarges constructed and developed in past two decades provide real potential for the portability of analytical instrumentation and the possibility of real-time, on-site measurements [4]. Lower operating costs associated with a lower consumption of consumables (e.g., working gases, electric current, and cooling water) are additional advantages of these miniaturized plasmas and discharges [4,7].

In 1993, Cserfalvi et al. [8,9] introduced a new, exotic concept into optical emission spectrometry (OES) analysis [i.e. the direct contact of atmospheric pressure glow discharge (APGD), with the sample solution through the usage of the electrolyte itself as the cathode in the dc discharge]. This resultant low-power, direct-current APGD (dc-APGD), generated between metallic anodes and cathodes that are electrolyte solutions overflowing inlet tubes or capillaries (electrolyte cathode discharge, ELCAD) or sprayed at the exit of capillaries toward counter electrodes (liquid-sampling APGD, LS-APGD), is nowadays considered one of the most promising and alternative excitation sources to

0165-9936/$ - see front matter © 2012 Elsevier Ltd. All rights reserved. doi:http://dx.doi.org/10.1016/j.trac.2012.09.002

traditional plasmas [i.e. inductively-coupled plasma (ICP) and microwave-induced plasma (MIP)] used in OES for the determination of different metals in water samples and other environmentally relevant liquid matrices [10–14].

Fig. 1 shows a characteristic glowing appearance and a zonal structure of such APGD systems with regions distinguished from a surface of an electrolyte solution to a metallic anode. Fig. 1 includes the cathode spot (CS) [i.e. the cathode surface covered by the discharge, the cathode dark space (CDS), the negative glow (NG), the Faraday space (FS), the positive column (PC), and the anode glow (AG)] [12].

Atomic and molecular excitation phenomena taking place in ELCAD and LS-APGD systems are primarily related to this zonal structure despite the small sizes and compact geometries of these discharges.

The uniqueness of both these dc-APGD approaches, which distinguishes them from ICP and MIP, is a convenient radiation characteristic of atoms emanating from this type of miniaturized excitation source. Relatively simple atomic emission spectra and a very low ionic emission, resulting in rare spectral overlaps, are distinctive characteristics of ELCAD and LS-APGD and make both excitation sources convenient for direct, online determinations of traces of metallic contaminations in different sample solutions [10,13–18]. The power density focused between electrolyte solutions and counter electrodes typically reaches 5–85 kW/cm^3 [19,20]. This is also one order of magnitude or more greater than the power density reported for commercial ICP sources, and directly relates to very low volumes of both discharges. Also, in most ELCAD applications, quantitative measurements with reasonably good detection power (from tens to single μg/L) and short-term precision (from few to several %) when using OES for the detection are possible under conditions of very low consumption of discharge gases or completely in the air with no gas supply [21]. The total electric power required to sustain such discharges is also very low (i.e. 22–82 W), and mostly dissipated in CDS that controls the evaporation rate at the gas-solution interface [17,18,20–23]. Analyzed sample solutions serve as liquid cathodes and therefore allow direct sampling and routine analyses in process control or environmental monitoring studies [17,18,20–23]. When coupled to mass spectrometry (MS), LS-APGD can be used as a low power, low sample-consumption ionization source, quite desirable due to the small amounts of oxide and hydroxide ions of elements produced [24,25].

In terms of simplicity of spectrochemical devices, discharge systems of dc-APGD generated in contact with the liquid electrode can easily be sustained and controlled with little effort and low operating costs [14,17,18,21,26–29]. The progress made in constructions of discharge cells made in recent years [14,18,20,22,23,30–36] and fundamental studies of spectroscopic properties of these microdischarges [17,21,29,36,37] surely indicate that it is possible to enhance the concentration of atoms in the discharge and

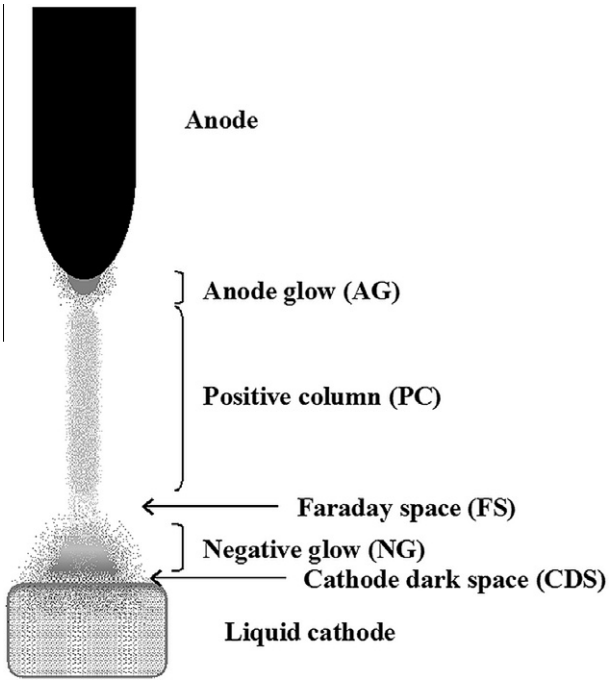

Figure 1. Discharge zones in direct current atmospheric pressure glow discharge (dc-APGD) generated in contact with a flowing liquid cathode (adapted from [9,30,36]).

improve, in this way, the analytical performance of this type of excitation source. All this makes the discharge a highly desirable excitation source in the spectrochemical analysis of environmental samples and measurements of trace elements present in these samples in a relatively straightforward, fast way.

The present article surveys the development in the past 20 years in the design of discharge systems for dc-APGD generated in contact with flowing electrolyte solutions, their analytical performance achievable under particular conditions and applications to the trace analysis of environmental and biological samples. We present and discuss the experimental conditions that affect the analytical response and the performance of this type of the excitation source. We also include analytical figures of merit evaluated for different discharge systems and their use in the analysis of real samples.

2. Operating mechanisms

Operating mechanisms of ELCAD and LS-APGD are important inasmuch as they allow understanding of atomization and excitation processes occurring in the discharge, showing the effect of experimental conditions on analytical performance and improving achievable figures of merit for these types of innovative excitation source.

The first operating mechanism, which is also the most important and frequently cited [8,9,11,13,16,17,20, 21,29,36,38–41], was proposed by Cserfalvi and Mezei [12,39] on the basis that the radiation characteristic of ELCAD is a consequence of the sputtering of the cathode electrolyte solution, the special, principal role of H_2O^+ molecular ions in secondary emission and three-body collisional processes occurring in the CDS of this discharge. Processes and reactions occurring in the discharge-electrolyte solution interface were more deeply discussed in previous reviews dedicated to ELCAD systems [40,41]. In brief, ELCAD is typically ignited in the air at the atmospheric pressure with a short spark or by approaching the anode to the surface of the flowing electrolyte solution (the cathode), but we need to consider that the discharge operates fully in a saturated H_2O vapor environment because the cathode is steadily sputtered by bombardments of its surface by positive ions [12,30,39]. CDS is the source of charge carriers produced through collisional ionization processes and the most important region of the discharge responsible for its self-ignition, further sustaining stable operation. When these positive ions collide with H_2O molecules of the cathode surface, the chemical composition of the electrolyte solution is changed through different ionization reactions included in a modified Hart-Anbar cycle [40,41]. This is accompanied by secondary electrons emitted from the cathode [12,39–41]. Subsequent production of H_2O^+ or OH^+ molecular ions in CDS saturated with the H_2O vapor is most probable and probably takes place through electron-impact ionizations {i.e. $H_2O + e = H_2O^+ + 2e$, or $H_2O + e = OH^+ + H + 2e$ [12,13,15,16,38]}. As a result, H_2O^+ and/or OH^+ molecular species are the predominant positive ions in CDS that subsequently transfer their energy through collisions with H_2O molecules [12,13,15,16,30,38]. Accordingly, the dissociative recombination of H_2O^+ molecular ions ($H_2O^+ + e = H + OH$) and/or the recombination of OH^+ molecular ions ($OH^+ + e = OH$) prevail. Oxygen ions (O^+), produced by the electron impact of the H_2O vapor, can also have an important role in processes occurred in this near-cathode zone (CDS) [16,38].

By and large, in all processes mentioned above, positive ions and electrons are generated and this leads to multiplication of charge carriers in CDS [39]. Due to this operating mechanism [11,16,38–41], positive ions of metals (M^+) leave the cathode because of the sputtering of its surface into CDS. However, they are unable to pass through this region because of its positive space charge. Hence, in the presence of a sufficient number of electrons [resulting from the ionization of discharge gases (i.e. the H_2O vapor, in addition to N_2 and O_2 from the ambient air) that have a suitably low energy for the recombination with M^+ ions], neutral metal atoms (M) are produced in three-body collisions involving one M^+ ion and two electrons. The rate of this process is inversely proportional to the average energy of electrons [38]. Neutral M atoms can subsequently diffuse to NG and be excited therein through the electron impact. Both these processes (i.e. the recombination in CDS and the electron impact excitation in NG) determine the intensity of atomic emission lines measured by OES [16,38]. However, this operating mechanism is still disputed, as the available data are rather inconsistent, affected mostly by experimental errors and lead to unfounded conclusions [42].

A more general neutral-release operating mechanism of processes occurring at the air-solution interface has been proposed for LS-APGD [25–28]. By a similarity to the operating mechanism of ELCAD, a special role of the H_2O vapor and air-originating species in launching and sustaining this discharge is stressed [24–28,43,44]. Apparently, it is deduced that the electrolyte solution can directly be vaporized into the discharge region by heating in the near-cathode zone (thermal release of droplets) and a release of solution droplets/vapors containing ions of elements [24–28,43,44]. Further evaporation of droplets, followed by dissociation of particulates and atomization of element species in the gas phase of the discharge, is possible because it has a certain thermal energy [24,25,27,28]. The excitation of atoms of elements in LS-APGD can happen through inelastic collisions with electrons and other energetic neutral species.

Both operating mechanisms describing phenomena taking place in the discharge (ELCAD and LS-APGD) are supported by very strong emission bands of OH molecules within the spectral range of 306–320 nm and originating from H_2O^+ and/or OH^+ precursor species [8–10,15,16,21,23,26,33,36–39]. Background MS spectra, obtained for LS-APGD used for the ionization, also reveal that different $(H_2O)_nH^+$ clusters (n = 6, 9, 12) are formed [24]. Atomic lines of the Balmer series of H are commonly identified [8,9,13,15,16,21,23,33,36–39]. In addition, as a result of the electron impact of H_2O vapor molecules, several O ionic lines (O II) can be observed in spectra of ELCAD operating in air and N_2 [15,38] or Ar [16]. When ambient air is used as the discharge gas, molecular band spectra of N_2, NO and NH molecules are observed in ELCAD and LS-APGD [8–11,15,16,21,23,26,27,36–38]. Surprisingly, Ar and He atomic lines are absent in emission spectra of ELCAD sustained in these

Table 1. Atomic and molecular species identified in emission spectra of the near-cathode region of direct-current, atmospheric-pressure, glow discharge (dc-APGD) systems generated in contact with flowing electrolyte solutions

OH	$A\ ^2\Sigma^+ - X\ ^2\Pi$ system with the following transitions:
	(0,0), (1,1) and (2,2) with overlapped band heads within 306.4–320.9 nm [8–10,15,16,21–23, 26–28,31,33,36,43,8[a],9[a],15[a],16[a],51[b],52[c],53[c],54[d]]
	(1,0), (2,1) and (3,2) with overlapped band heads within 281.1–289.9 nm [8,15,16,21,23,26,27,36,37,51[b],52[c],54[d]]
	(2,0) and (3,1) with overlapped band heads within 260.0–269.1 nm [21,23,51[e]]
N_2	$B\ ^3\Pi - A\ ^3\Sigma$ first positive system with the following transitions:
	(4,2) with the band head at 750.4 nm [26,27]
	(7,4) with the band head at 654.5 nm [26,27]
	(6,2) with the band head at 607.0 nm [26,27]
	$C\ ^3\Pi - B\ ^3\Pi$ second positive system with the following transitions:
	(0,3) with the band head at 405.9 nm [21–23,38,51[b],54[d]]
	(1,4) with the band head at 399.8 nm [36,37]
	(2,5) with the band head at 394.3 nm [36,37]
	(3,6) with the band head at 389.5 nm [36,37]
	(0,2) with the band head at 380.5 nm [10,15,21,23,36,37,49[e],54[d]]
	(1,3) with the band head at 375.5 nm [36,37,49[e]]
	(2,4) with the band head at 371.0 nm [36,37]
	(3,5) with the band head at 367.2 nm [36,37]
	(0,1) with the band head at 357.7 nm [8–10,15,16,21,23,36,37,39,49[e],54[d]]
	(1,2) with the band head at 353.7 nm [36,37,49[e]]
	(2,3) with the band head at 350.0 nm [36,37]
	(0,0) with the band head at 337.1 nm [10,15,21,23,31,36,37,51[b],54[d]] overlapping with NH
	(1,0) with the band head at 315.9 nm [36,37] overlapping with OH
	(2,1) with the band head at 313.6 nm [36,37] overlapping with OH
	(2,0) with the band head at 297.7 nm [36,37]
	(3,1) with the band head at 296.2 nm [36,37]
	(4,2) with the band head at 295.3 nm [36,37]
N_2^+	$B\ ^2\Sigma^+ - X\ ^2\Sigma^+$ first negative system with the following transition:
	(0,0) with the band head at 391.4 nm [37]
	(1,0) with the band head at 358.2 nm [8–10,16] overlapping with N_2
NH	$A\ ^3\Pi - X\ ^3\Sigma^-$ system with the following transitions
	(0,0) and (1,1) with band heads at 336.0 and 337.0 nm [8,9,15,16,26,27,36,37,43,52[c]] overlapping with N_2
NO	$A\ ^2\Sigma^+ - X\ ^2\Pi$ third positive system with the following transitions:
	(0,3) with the band head at 259.6 nm [36,37]
	(0,2) with the band head at 247.9 nm [36,37]
	(0,1) with the band head at 237.0 nm [36,37]
	(0,0) with the band head at 226.9 nm [36,37]
	(1,0) with the band head at 215.5 nm [36,37]
	(2,0) with the band head at 205.3 nm [36,37]
H I	434. 1 nm overlapping with N_2 [36,37], 486.1 nm [8–10,15,16,21,23,31,33,36–38,49[e],51[b],52[c],53[c]], 656.2 nm [16,21,23,36,37,49[e],51[b],52[c],53[c]]
O I	777.2 nm, 777.4 nm and 777.5 nm [21,23,36,37,52[c],53[c]], 844.6 nm [36,37,52[c]]
O II	441.5–441.7 nm [15,16,21,23,31,38], 459.1 nm [21,23,38], 459.6 nm [21,23,38], 463.9–464.2 nm [16,21,23,38], 467.4–467.6 nm [21,23,38],466.6–469.9 nm [15,21,23,38], 470.7–470.8 nm [15,21,23,38]

[a] Observed in the second order.
[b] For alternating current electrolyte atmospheric liquid discharge (ac-EALD).
[c] For liquid electrode-dielectric barrier discharge (LE-DBD).
[d] For liquid film-dielectric barrier discharge (LF-DBD).
[e] For a miniaturized electrolyte cathode discharge (ELCAD) system.

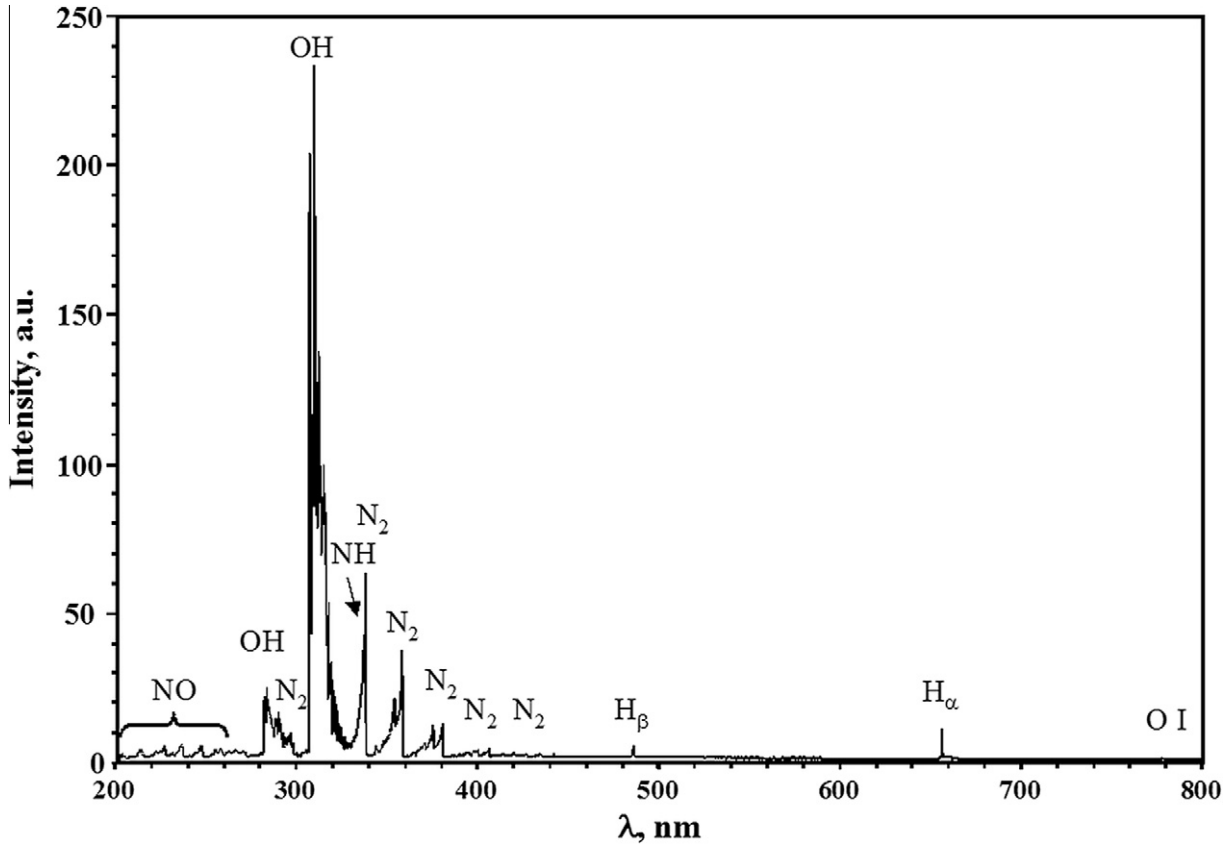

Figure 2. A typical emission spectrum of direct current atmospheric pressure glow discharge (dc-APGD) generated in contact with a flowing liquid cathode (water acidified to pH 1.0).

noble gases [16]. This is because the electrolyte solution acts as one electrode body of the discharge and its vaporization produces all discharge components (i.e. atomic and molecular species) to such a degree that the atmosphere of other gases has no effect on the emission spectra [45]. Table 1 gives the atomic and molecular species identified in spectra (see Fig. 2 for the 200–800 nm spectral range) of different dc-APGDs generated in contact with flowing electrolyte solutions.

3. Electrode-discharge systems

3.1. ELCADs

Two kinds of ELCAD system are described in the literature {i.e. closed and semi-closed cells [8,9,11–13,16,22,38,39] and open-to-air cells [10,15,17,18,20,21,23,29–37]} (see Fig. 3).

The first type introduces air, N_2, Ar and He as discharge gases at pressures lower and higher than atmospheric (i.e. within 200–1200 mbar [13,16,22,38,39]. In cell arrangements with vents, electrodes are opened to the ambient air, and such an approach prevents sudden and periodical changes in the atmospheric pressure or the condensation of the H_2O vapor inside [8–10,15]. Extra flows of air can be introduced into these cells continuously to prevent accumulation of H_2 and O_2 in the gas phase of the discharge [10,15].

Glass or glass-plastic bodies or housings are usually used to construct ELCAD cells. They hold metallic anodes at the top of cells, have inlet tubes for electrolyte solutions, can discharge or venting gases, axially view the discharge and record the emitted radiation [8–13,15,16,20,22,30–39]. In cathode compartments, usually located at the bottom of cells, electrolyte solutions are continuously introduced through centrally-placed inlet tubes made of glass or quartz [8–13,15,16,22,31,33,38,39], plastic [15] or stainless steel [32]. Quartz tubes inserted into external graphite tubes can provide the electrical contact [20,36,37]. In the construction proposed by Webb et al., solutions enter the cell through a glass pipette or a micropipette bent at the end and immersed in a bulky reservoir completely filled with electrolyte solution, so their tips are raised ~2 mm above the edge of the reservoir [17,18,21,23,29]. Also, rectangular black polyethylene dividers are used in these systems in order to reduce the amount of H_2 produced in the vicinity of the graphite electrodes and to reduce the background level by blocking the discharge from other external light sources [17,18,21,23,29].

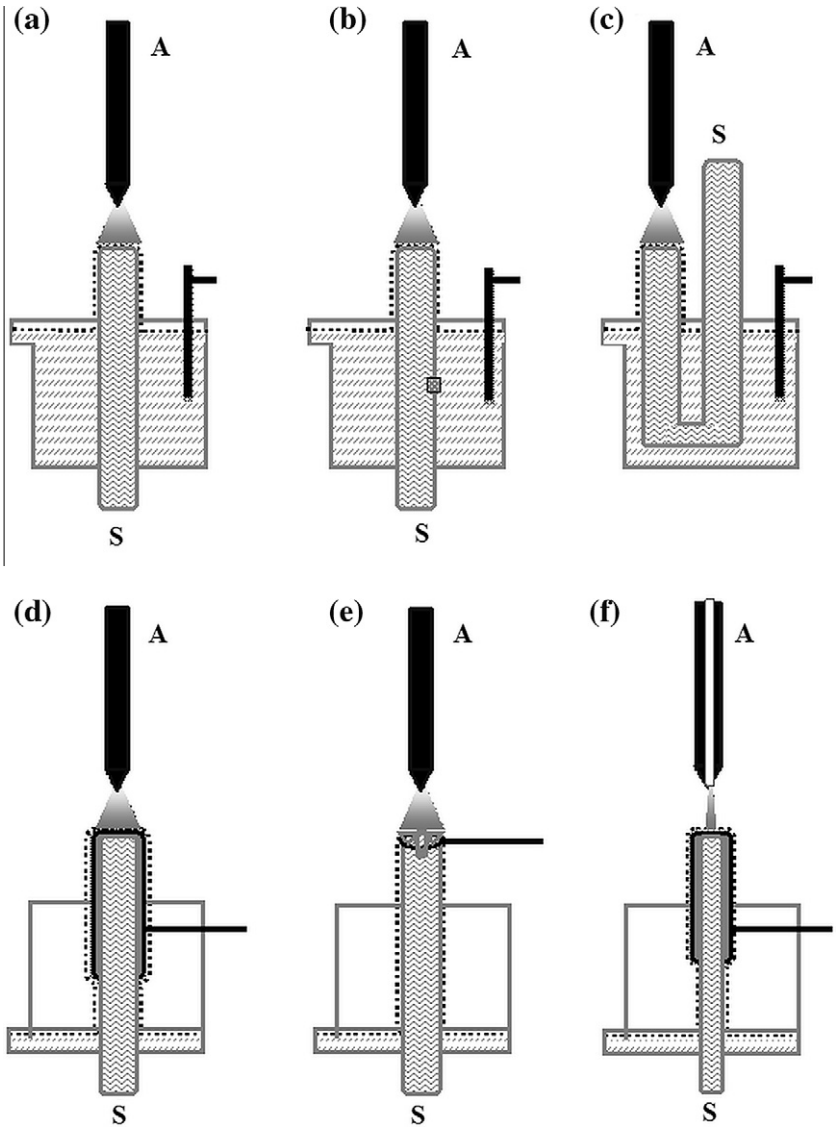

Figure 3. Different electrolyte cathode discharge (ELCAD) cell constructions used in: (a) [8–11,13,15,16,38,39,45]; (b) [12,22,30,31]; (c) [17,18,21,23,29]; (d) [20,36]; (e) [33,34]; and, (f) [37]. A, Anode; S, Electrolyte solution (liquid cathode).

In earlier ELCAD devices, inlet tubes had relatively high internal diameters or were even extended at the top [8,9,11–13,38,39]. In these conditions, the electrolyte-cathode surface was higher than the CS formed above the inlet tube and a normal type of the discharge was realized. In other cases, inlet tubes of small internal diameters or capillaries introduced electrolyte solutions [10,12,15–18,20–23,29–37]. As a consequence, electrolyte-cathode surfaces at the end of these tubes or capillaries are covered by the discharge and an abnormal type of the discharge is produced, for which the voltage increases with the discharge gap at a given current, while the current increases with the voltage at a certain discharge gap.

The overflowing electrolyte solution is important to maintain the electric contact in all ELCAD arrangements. It is usually collected at the bottom of cells, forming cathode reservoirs or pools [8–13,16–18,21–23,29–31,33,38,39]. Outlet tubes of electrolyte solutions are usually placed at bottom [8–10,15,16,22,30,31] or top [20,33–37] of these reservoirs. Outlet tubes for solutions are also inserted inside cells at a certain height to ensure a constant level of electrolyte solutions and an outlet for both discharge gases and electrolyte solutions [11–13,32,38,39]. Solutions can also directly overflow from the reservoir so the level of the electrolyte is held constant [17,18,21,23,29]. For a smoother overflow of electrolyte solutions and a greater stability of the discharge, glass delivery tubes are modified (i.e. through a V-groove cut on the top of the tube) [33–35].

A dc high-voltage (HV) ground connection at the negative potential of the discharge circuit is normally

supplied to electrolyte solutions through electrodes {Pt [10,12], graphite [8,9,16–18,21,23,29] or stainless steel [11–13,38,39]}. In most cases, electrodes are directly inserted into cathode compartments (with overflowing electrolyte solutions) or, to prevent the introduction of H_2 evolved to the discharge, placed in separate chambers that are connected with the main compartments of the cathode [8,9,16]. Wires made of Pt can also be used to provide the electrical contact; they are inserted into a quartz inlet tube at its upper part [15] or simply into the cathode compartments [22,30,31] or connected to an external graphite tube [20,36,37]. When a stainless-steel inlet tube is used, its direct connection to the ground is possible [32]. A Pt ring placed below the top of a glass inlet tube, through which the electrolyte solution overflows, can also provide the ground potential to the electrolyte solution cathode [33–35]. Finally, the electrical contact of the flowing electrolyte solution with the rest of the cathode in a reservoir can be provided through an ionic conductor placed in a hole of the inlet capillary [12,22,30,31]. In this case, slower electrolyte-solution flow rates can be used.

Anodes are always vertically mounted just above the surface of overflowing solutions in a line with inlet tubes and connected to the positive dc HV potential. They are commonly made of W [8,9,11–13,22,30,33–35,38,39], Pt [10,15,16], Ti [17,18,21,23,29] or, rarely, Mo [20,36] and stainless steel [32]. An Ar microjet, where a miniature gas flow is introduced through a steel nozzle, can also act as the anode [37].

3.2. LS-APGDs

LS-APGD is much simpler in construction and required components than ELCAD [19,24–28,43,46] (see Fig. 4), although some authors do not regard it as an electrolyte electrode discharge, like ELCAD, as it runs between two metal electrodes and can consume all the sample flow or be operated with a reverse polarity [41]. LS-APGD is typically sustained between the surface of the solution flowing from stainless-steel capillaries [19,26–28,44,46] or glass capillaries [24,25,43] and opposite to rods of Cu [26,27,43], Ni [19,28,43,44,46] or stainless steel [43], which serve as counter electrodes. Both electrodes are mounted on horizontal translation stages, fully opened to the ambient air and with no windows or containment structures. Ni counter electrodes can also be placed perpendicular to the end of the opening of inlet capillaries [24,25,43].

Both electrode arrangements in LS-APGD cause electrolyte solutions to be almost totally consumed. Apparently, when flow rates of electrolyte solutions lower than 1.5 mL/min are used, very little solution drips from inlet

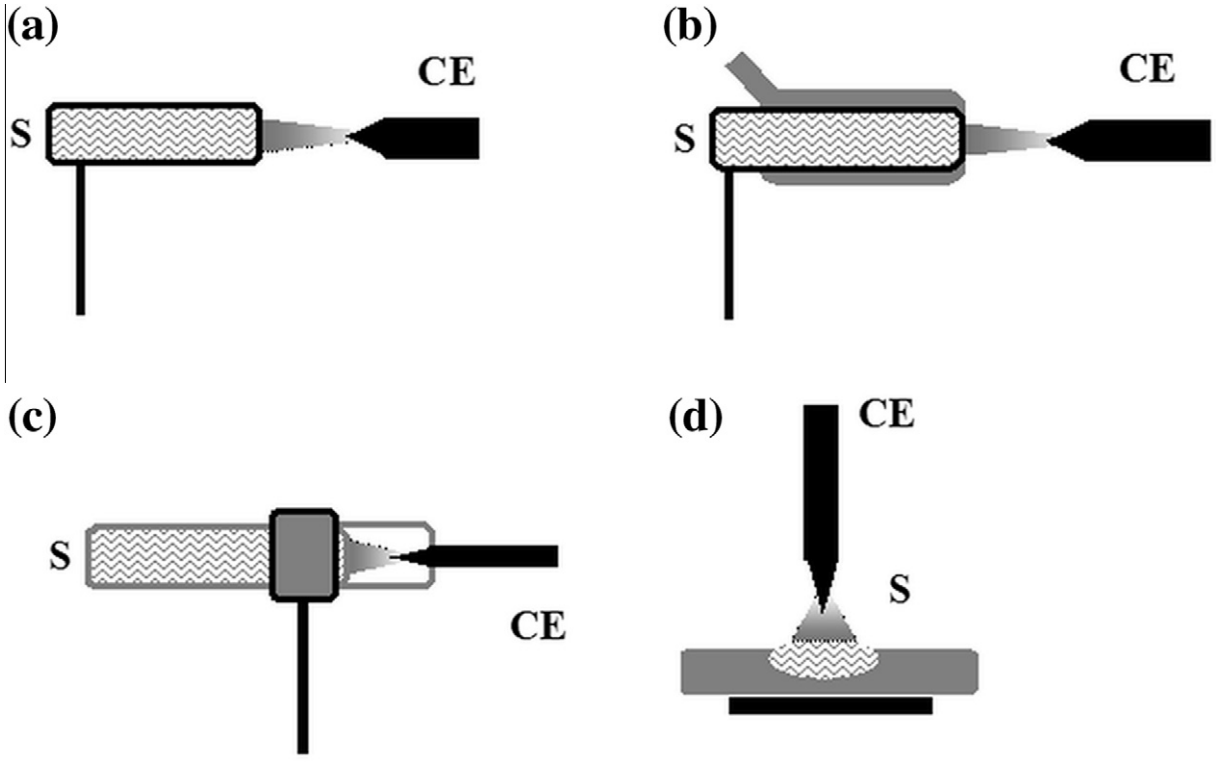

Figure 4. Liquid electrode discharge systems: (a) LS-APGD [26]; (b) LS-APGD with a sheath gas [19,24,25,27,28,43,44,46]; (c) LE-DBD [52,53]; and, (d) LF-DBD [54]. LS-APGD, Liquid sampling-atmospheric glow discharge; LE-DBD, Liquid electrode-dielectric barrier discharge; LF-DBD, Liquid film-dielectric barrier discharge (LF-DBD); CE, Counter electrode; S, Electrolyte solution.

capillaries [26,27]. At flow rates of 0.1–0.5 mL/min or less, electrolyte solutions are totally consumed with no liquid waste generated, while, at the coincidentally low discharge currents used, a fine aerosol is generated [19,24,26,27,43,44]. However, in the latter case, coaxial flows of N_2 [27,28,44], He [19,28,43,46] or Ar [24,25] sheath gases, introduced through other stainless-steel tubes surrounding the solution inlet capillaries, are incorporated to improve the transport efficiency of electrolyte solutions toward counter electrodes and alleviate unstable operation of the discharge resulting from pulsations of electrolyte solutions. These auxiliary gas flows also efficiently cool inlet capillaries and counter electrodes [27,28,44].

Compared to ELCAD, LS-APGD can be operated stably using flowing electrolyte solutions as cathodes (connected to the negative dc HV potential and grounded) or anodes (connected to the positive dc HV potential and grounded) [26–28,43]. The first configuration is called the solution-grounded cathode (SGC) and is identical in terms to the electrical connection to ELCAD. The reversed polarity configuration is called the solution-grounded anode (SGA). Metallic rods can also be grounded while electrolyte solutions are powered differently, giving two other LS-APGD configurations [i.e., the solution-powered cathode (SPC) and the solution-powered anode (SPA)].

Despite so many combinations, the transport of elements into the discharge regions is the most efficient when electrolyte solutions act as the SGC, probably due to the direct volatilization of the solution at the capillary exit [26–28]. As a result, the greatest emission intensity of atoms of various elements is observed in the SGC configuration, although the SGA configuration allows better stability and reproducibility of the analytical response [28]. A very recent study showed that SGA, although it provided comparable intensities for atomic emission lines compared to SCG under different experimental conditions, is much better for sample-to-sample reproducibility and maintaining lower background levels responsible for better detection power [43].

3.3. Other systems

An interesting closed-type U-shaped ELCAD cell, used as a sputtering source in an ICP instrument instead of a pneumatic nebulization (PN) unit, is described by Cserfalvi and Mezei [45]. In this system, a Pt electrode is immersed in the electrolyte solution in one arm of the tube to supply the electric contact, while a W anode is approached to the surface of the electrolyte-solution cathode in the second arm of the tube. The surface of the liquid cathode is renewed by a steady flow of the electrolyte solution through the bottom of the U-tube at 5.0 mL/min, while all generated products are swept to an ICP torch by a stream of Ar (1.0 L/min). Zhu et al. report an even simpler, smaller device for that purpose [47]. Sample solutions are introduced (at 2.5 mL/min) into a closed-type cell through a glass capillary, overflow and gather at the bottom of the cell, forming a solution reservoir, in which a graphite electrode is immersed. The discharge is sustained between the outlet of the capillary and a W anode, placed opposite the capillary. The electrical contact between the discharge and the solution is provided by its overflow. All products generated by ELCAD, particularly Hg vapors, are swept along by an Ar stream (0.5 L/min) to an ICP torch through a gas-liquid phase separator.

Attempts have also been made to miniaturize the ELCAD excitation source by using microfabrication techniques and producing lab-on-chip devices [48,49]. Such devices are fabricated in glass and inserted between a stream of the electrolyte solution flowing (at 10–100 μL/min) within one microchannel and a Pt-wire anode immersed in the opposite channel. Ar flow, introduced through another microchannel, perpendicular to the discharge channel, is used to provide the discharge atmosphere. In this approach, the total power consumption is very low (i.e. below 1 W).

An open-air microglow ELCAD apparatus with a non-flowing electrolyte solution cathode and a graphite anode has also been proposed [50]. A capillary tube reservoir with an immersed stainless steel connection is manually filled with solution. After supplying a breakdown voltage of 2.0–2.5 kV, depending on the composition of solutions, the discharge is sustained within 15 s while the sample solution inside the reservoir is consumed (about 300 μL). The total power consumption of this system is about 5–6 W.

The alternating current (ac) ELCAD, named electrolyte atmospheric liquid discharge (ac-EALD), was reported by Huang et al. [51]. In this case, a glowing discharge between a W rod and the surface of an electrolyte solution delivered at 0.25 mL/min through a capillary is sustained after supplying the ac HV (3700 V, 30 kHz). The total power consumption is 18 W. The solution overflows from the capillary, provides the electrical contact with the rest of the solution, is kept at a constant level in a reservoir and is connected to the circuit through a graphite electrode immersed inside.

Interestingly, specially-designed capillary liquid-electrode (LE) [52,53] or liquid-film (LF) [54] dielectric barrier discharges (DBDs) are also described in the literature (see Fig. 4). Both discharges operate at low power in the ambient air.

4. Effect of operating conditions on the analytical response

The intensity of atomic and ionic spectral lines of elements acquired in spectra of ELCAD or LS-APGD systems are established as depending on the rate of recombination processes taking place in CDS related to the average energy of electrons available in this region [11,38]. The

latter feature is strictly associated with operating parameters of the discharge (i.e. the cathode fall, the discharge voltage, the discharge current, the discharge gap, the pH of the cathode electrolyte solution, as well as the pressure and the composition of the discharge gas) [15–17,20,21,29,36,38]. In LS-APGD, the analytical response of the discharge can also be treated as a result of various processes, including nebulization, desolvation, vaporization, and excitation, being a function of the discharge current, the flow rate of the electrolyte solution and the flow rate of the sheath gas [25].

4.1. Discharge gas and its pressure

In all open-type cell ELCAD devices and all LS-APGD configurations, the discharge is sustained in the ambient air at atmospheric pressure [8–11,15,17,18–21,23–29,32–36,38,43,46]. In closed-type cell ELCAD systems, except for air [13,16,38,39], other gases {e.g., N_2 [13,38,39], Ar [16] and He [16]} are applied as discharge gases and continuously introduced into discharge cells at varying pressures and flows. In these systems, apart from sustaining the discharge, gas flows additionally help to avoid condensation of the H_2O vapor on quartz windows of cells [13,38,39]. Apparently, changes in the pressure of the discharge gas in these systems affect the analytical response [13,38]. A gradual increase in the pressure of air from 665 mbar to 1200 mbar results increases the population of low-energy electrons and, as a consequence of the operating mechanism of ELCAD, an intensification of dissociative recombination processes of positive molecular ions and a rise of the cathodic current density [13]. Thus, intensities of several atomic and ionic emission lines {i.e. Ca II 393.4 nm, Cd I 228.8 nm, Na 589.9 nm, and Zn I 213.8 nm} tend to increase from almost zero (at 665 mbar) to their maximal values (at 1200 mbar) [38]. The increase in the intensity of the OH band with the pressure is also significant. This is probably due to the recombination of precursor H_2O^+ and/or OH^+ molecules in these conditions [38]. Intensities of H I 486.1 nm and O II 441.5 nm lines decrease in these conditions, due to high values of their upper energy levels [38].

4.2. Discharge voltage and current

dc HV applied to electrodes in all ELCAD and LS-APGD systems is high {i.e. 550 V [32], 750 V [33,34], 760 V [35], 850 V [12], 950 V [31], 1000 V [18,23], 1020 V [22], 1050 V [15,21], 1200 V [11,13,30,38,39], 1250 V [27] or even 1500 V [9,10,16,20,36] or 1700 V [28,46]. One or two ballast resistors are commonly connected in series with electrodes to stabilize the current flow and to maintain the steady operation of the discharge. The gap between the anode (the metallic rod) and the cathode (the surface of the electrolyte solution), the so-called discharge gap, is typically 1–6 mm [8,10,11,15–17,19–23,26–31,33–36,43,46]. Much lower discharge gaps are also possible {e.g., 0.7 mm [18,32] or 0.5 mm [36]}. This means that the volume occupied by this type of the discharge is extremely small, only a few mm^3 or less [20].

After applying dc HV to electrodes and initializing the discharge, the discharge current flowing through them is 50–85 mA [8,10,12,13,16–19,21–23,27–31,33–35,38,43,46]. Higher discharge currents {i.e. 90 mA [38], 95 mA [30], 100 mA [39], 110 mA [15] and even 130 mA [15]} or lower discharge currents {i.e. 40 mA [26,27,32] and 20 mA [20,36]} are also used.

When the discharge gap is increased, the discharge voltage increases [15,16,20,23,26,32,36]. As a result, intensities of atomic emission lines (e.g., Cd I 228.8 nm, Cu 324.7 nm, Mg I 285.2 nm, and Zn I 213.9 nm) may increase at the beginning but then remain unchanged and/or fall [20,21,23], or immediately decrease from the beginning [36]. Also, greater fluctuations and the susceptibility of the discharge to air currents at higher discharge gaps were noticed [23]. This is responsible for worsening the analytical performance [i.e. higher values of relative standard deviation (RSD) for the precision and limits of detection (LODs)].

The effect of the discharge current on the analytical response of ELCAD and LS-APGD is significant. The intensity of many atomic and ionic emission lines (i.e. Ca II 393.4 nm, Ca I 422.7 nm, Cd I 228.8 nm, Cr I 357.8 nm, Cr I 425.4 nm, Cu I 324.7 nm, Fe I 248.3 nm, H I 486.1 nm, Hg I 254.4 nm, K I 766.5 nm Mg II 279.6 nm, Mg I 285.3 nm, Na 589.0 nm, Ni I 341.5 nm, Pb I 368.5 nm, Pb I 405.8 nm, and Zn I 213.9 nm) increase when the current increases from 30 mA to 110 mA or even 140 mA [8,10,15,16,21,26–28,38]. Such behavior of atomic emission lines may be attributed to the size of CS that gets bigger at higher discharge currents [8,12,15,16]. Also, bearing in mind the operating mechanism of ELCAD, we can assume that the number of positive ions bombarding the surface of the electrolyte solution is higher while the average accelerating potential of ions, caused by the concomitantly higher discharge voltage, also increases [15,16]. Considering the energy of the discharge, it seems that the increase in the discharge current provides more efficient vaporization of sample solution and sputtering rate of elements. Hence, it increases the number of atoms of these elements along with the number of electrons available to excite them in NG [25–28].

In general, the emission from all discharge regions rises in these conditions [21]. However, very high discharge currents (i.e. above 120 mA) may be responsible for unstable operation of the discharge, since a larger fraction of the energy is focused at the air-solution interface and results in the enhanced vaporization of H_2O [10,15]. Enhancement of the intensity of ionic emission lines is slight or completely independent of the discharge current [9].

When LS-APGD is used as the ion source in elemental MS, high discharge currents, normally used in OES measurements, are inappropriate. They lead to intense production of different H_2O-related clusters yielding a relatively high background level in mass spectra [24,25]. For that reason, operation of LS-APGD at relatively low discharge currents (5–10 mA) is favored because more ions of elements and less H_2O-containing species contributing to the background level are produced, but the discharge may not operate in the total-consumption mode [24,25].

4.3. Electrolyte-solution flow rate

The flow rate of samples in earlier ELCAD devices is relatively high (i.e., 5.0–10.0 mL/min) to ensure a continuous overflow of electrolyte solutions, the electrical contact and a stable and constant distance between electrodes [10,11,13,15,16,38,39]. High flow rates also reduce the boiling of H_2O. Lower flow rates of electrolyte solutions (<5.0 mL/min) are accompanied by continuous fluctuations in drop formation at the top of inlet tubes [33]. The inter-electrode distance changes in these conditions and the discharge flickers [33]. Resultant variations of the background cause deterioration in the detectability of the system [33].

The use of capillaries and tubes of smaller diameters or special ways to supply the dc HV negative potential to electrolyte solutions in later ELCAD constructions resulted in lower flow rates of electrolyte solutions being used {i.e. 0.6–6.2 mL/min [18,20–23,30–32,36]}. Nevertheless, in selecting optimal solution-uptake rates, scientists had to consider their significant effect on the intensity of atomic emission lines [20,21,32,36] or values of LODs [22]. In general, as shown by several atomic emission lines (i.e. Ca I 422.7 nm, Cd I 228.8 nm, Cu I 324.7 nm, Mg I 285.2 nm or Zn I 213.9 nm), the intensity of these lines increases with the increase in the electrolyte-solution flow rate, but then settles down or rapidly decreases as a consequence of a higher contribution of the H_2O vapor in the near-cathode zone [20,21,32,36]. The H_2O vapor mentioned or its products may reduce the energy and/or the number of electrons available for the excitation of atoms [20,21,36]. Coincidentally, the intensity of emission bands of OH [21,36] and N_2 [36] molecules in addition to atomic O and H lines [36] becomes stronger in these conditions. When relatively low flow rates (0.8–2.6 mL/min) are applied in modified inlet tubes [18,22,33–35], the use of electrolyte carrier solutions is quite low and discrete sample amounts can be introduced into the discharge by means of a flow-injection (FI) mode {i.e. 100 μL [35], 37 μL [22] or 25 μL [18]}.

In LS-APGD, electrolyte solutions are delivered at low flow rates not greater than 1.5 mL/min {e.g. 1.0 mL/min [26,27], 0.4 mL/min [46], 0.3 mL/min [25,27,28,43,44], 0.1 mL/min [24], 0.08 mL/min [44], 0.02 mL/min [19] or even 0.01 mL/min [25], and are almost totally consumed by the discharge. When electrolyte solutions are delivered at flow rates less than 0.5 mL/min and an extra co-axial sheath gas flow is passed, the formation of a fine aerosol can be observed at the end of inlet capillaries, enhancing nebulization and vaporization of electrolyte solutions [19,26–28,46]. These systems are especially well suited to the introduction of discrete samples in the FI mode using injection loops of 5-μL [25–28,44], 20-μL [46] or 50-μL [24,43]. Unlike ELCAD, lower solution flow rates have rather positive effects on the analytical performance of the discharge {e.g., higher intensities of Hg I 253.7 nm line, due to a lower dampening of the discharge and a better vaporization of solution droplets). Less H_2O vapor in the near-cathode region of the discharge does not consume the discharge energy [28]. It is especially important in application of LS-APGD as the ion source in MS [24,25].

4.4. Electrolyte-solution pH

Electrolyte-solution pH is one of the most critical parameters that affect the intensity of atomic emission lines of elements of different excitation energies (1.6 eV and 12.8 eV in Li and H, respectively) due to its vital role in processes of the sputtering of the electrolyte solution, the excitation of discharge and its stable operation, as both ELCAD and LS-APGD [8–10,15–17,20,21,26–28,33,36,38,39,46]. Normally, a decrease in solution pH from high values to about 0.0–1.0, caused by an increase in acid concentration, results in a significant increase in the intensity of atomic emission lines of various metals and a much more stable operation of the discharge at relatively lower discharge voltages [8–10,15,20,26,36,38,46]. Even the H_β line is more intense when the pH of electrolyte solutions decreases [8,36,38]. With the OH molecule, the intensity of its band head increases [36] or does not significantly change [21]. A similar trend is observed in the intensity of the band head of the N_2 molecule [36]. Conversely, the intensity of the band head of the NH molecule steadily decreases when the pH of the electrolyte solution decreases to 1.0 [39].

The reason for very low intensities of atomic emission lines or their complete absence in emission spectra at the pH of electrolyte solutions above 2.5–3 is presumed to result from high values of the cathode fall settled in these conditions [8–11,21,39]. As a consequence, the energy of free electrons increases and recombination processes in CDS responsible for the neutralization of element ions is suppressed [11]. However, changes of the vertical distribution of atomic emission lines within the distance between electrodes may suggest that the effect of pH is more complicated [21] than that anticipated on the basis of the operating mechanism given [39]. Accordingly, it appears that changes in the conductivity of electrolyte solutions are also important [21,46]. A high conductivity of electrolyte solutions (low pH) results in an easier

consumption of the majority of the power supplied to the discharge in the gas phase [46]. In the opposite situation (low conductivity, high pH), the greater energy can be focused at the gas-solution interface, and enhanced heating of the electrolyte solution and vaporization of H_2O manifest this [46]. In these conditions, additional amounts of the H_2O vapor are introduced into the discharge and the excitation mechanism is quenched [46]. Hence, the operation of ELCAD and LS-APGD at pH of 2.0 or higher is typically accompanied by serious fluctuations in the appearance of the discharge and the radiation emitted [46]. It simply gets narrower and its intensity reduces [15] or its structure even collapses [46].

The optimal values of pH, which provided the lowest values of the cathode fall (500–550 V) and the highest intensities of atomic emission lines of different elements, were 0.0 [19,24,25,36], 0.7 [33–35], 0.9 [21], 1.0 [8,10,15–18,20,23,26–29,32,37,44,46,55] or 1.5 [9,13,38,39] or 1.6 [22,31]. However, according to data reported by Khlyustova et al. [55], even in an alkaline medium (pH 12.0), intensities of atomic emission lines of Ca, Li and Na are only somewhat lower than those in an acidic medium (pH 1.0). Electrolyte solutions are commonly adjusted to appropriate pH values using HNO_3 [10,15–19,21,23,24–29,32–35,44,46] because of a chemical compatibility of this acid with sample-preparation procedures used for the analysis. Other acids {i.e. H_2SO_4 [8,9,29,39] or HCl [13,20,22,29,31,36–38,44,5]} are also applied, but less frequently. With HCl, its presence can be responsible for higher or considerably higher intensities of the Cd I 228.8 nm line, compared to those obtained when electrolyte solutions are acidified with HNO_3 or H_2SO_4 [11], supposedly related to the effect of Cl^- ions in the recombination processes with metal ions in CDS and the production of neutral atoms [11]. The type of acid (HCl, HNO_3, H_2SO_4, or HF) used for acidification of the electrolyte solution can be of immense importance to the conductivity of electrolyte solutions and the analytical performance [33]. It seems that only electrolyte solutions acidified with HCl and HNO_3 have the highest conductivity and produce in this way the maximum analytical response (i.e. intensities of Cu I 327.4 nm and Hg I 253.7 nm lines) [33]. What is more, the increase in the concentration of HCl and HNO_3 from 0.05 mol/L to 0.30 mol/L [33,35] or the concentration of HCl in the range 0.01–0.06 mol/L [11] or 0.1–1.0 mol/L [20,36] commonly results in a steady increase in intensities of atomic emission lines of various elements (i.e. Cd, Cu, Hg, Mg, Ni, Pb and Zn). However, the best precision, reflected by the reproducibility of signals, is normally obtained within the range 0.05–0.20 mol/L due to lower fluctuations of the cathode surface in the upper part of solution-inlet tubes [20,33,35,36].

Interestingly, LS-APGD can be operated with not only acidic solutions but also low concentrated solutions of Li and Na ions, but the analytical response achieved in the latter case is lower than that obtained in the presence of H_3O^+ ions [26,27], because electrolyte solutions containing H_3O^+ have lower boiling point and ionization potential [26,27].

5. Chemical interferences and the effect of additional reagents

Different concomitants present in electrolyte/sample solutions at elevated levels can affect the conductivity of these solutions, the substrates in recombination processes or the sources of additional electrons. In this way, their presence can alter the course of atomization and excitation processes in the discharge and influence the analytical response. Accordingly, the effect of the addition of Cl_2, CH_3Cl or $CHCl_3$ to the air discharge atmosphere used in ELCAD on its analytical performance is significant and mostly related to the recombination of metal ions resulting from the solution cathode sputtering with negative Cl^- ions produced in these conditions [11]. In a similar way, Cl^- ions originating from HCl used for the acidification of electrolyte solutions are responsible for enhancing the intensities of atomic emission lines of Cd [11]. Unfortunately, PO_4^{3-} ions (added as H_3PO_4 or Na_2HPO_4) in electrolyte solutions are the source of matrix effects in measurements of Ca, and there is a marked drop of the response for this element obtained with ELCAD [17,18]. The addition of La salts, recognized to release Ca ions by preferentially binding PO_4^{3-} ions in flame atomic absorption spectrometry (FAAS), is unfortunately ineffective. What is more, La^{3+} ions produce matrix effects on Ca [17]. An increase in the discharge gap [17] or the use of a FI sample introduction arrangement [18] can be a remedy in this case.

Easily ionized elements (EIEs), including Ca, K, Li, Mg and Na, are quite often present in environmental and biological samples in relatively high amounts, so they can change excitation conditions in ELCAD and affect the analytical response for other elements. It is assumed that high concentrations of EIEs can lower the solution resistance and the solution heating, which both lead to a decrease in the transport of elements and the desolvation efficiency (e.g., by a deterioration in droplet formation and size) [17]. EIEs can also change the resistance of the discharge, its conductivity and excitation conditions (i.e. by an increase in ion and electron populations) [17,20].

Indeed, high concentrations of EIEs (170 mg/L of Li, 570 mg/L of Na and 980 mg/L of K, all separately added) in electrolyte solutions are responsible for a decrease in intensities of Cd, Cu and Mn atomic emission lines by 20%, 60–80% and 80–90%, respectively, in Li, Na and K [17]. Less suppression of Cd, Cu and Mn signals in the presence of 570 mg/L of Na (by 20% on average) is attained when a capillary delivery tube is used [23]. The

use of the capillary delivery tube and an FI arrangement in the same system can improve signals for Cd, Cu and Mn accompanied by the same content of Na by another 10–20% [18]. The presence of relatively high concentrations of Na (up to 200 mg/L) is usually tolerable and does not result in changes of intensities of atomic emission lines of Cd, Mg and Zn [20]. Above this concentration, the analytical response for Cd, Mg and Zn is suppressed, probably due to the increase in electron density [20]. The effect of Na on the emission of Ca is also substantial [17]. With Mg, its presence in the solution has no effect on the intensities of atomic emission lines of Cd and Zn up to 200 mg/L, then, above this concentration, signals of Cd and Zn increase [20].

It seems that the form in which EIEs are present in the electrolyte solution also matters. Apparently, K ions present in the electrolyte solution varied in concentration in the range 390–5900 mg/L, but, when added as KCl, KNO_3 or K_2SO_4, produced a gradual decrease in the intensity of the atomic emission line of Cd above 780 mg/L with KNO_3 and K_2SO_4 [11]. With KCl, the response for Cd remained practically unchanged, possibly due to a compensation effect resulting from the presence of Cl^- ions [11]. By contrast, the presence of NH_4^+ had no effect (Cd) or enhanced the response for elements by 10% (Cu) and 40% (Mn) [17].

Usually, the effect of EIEs on the background level (continuum spectra) in the vicinity of atomic emission lines of elements is similar to that for these lines themselves – when intensities of these analytical lines are suppressed or enhanced, the intensity of the background more or less behaves in the same way [17].

With LS-APGD, high concentrations of K and Ca ions in electrolyte solutions (up to 1000 mg/L) practically have no significant influence on the response for Cu, Sc, Mo and Hg acquired by OES [46]. Very high concentrations of Ca and Na salts result in instability of LS-APGD due to its ''shoring out'' [46]. These salts may also affect vaporization of the electrolyte solution [46]. When LS-APGD is applied as the ion source in MS, the effect of Na ions (added as NaCl) at the concentration up to 500 mg/L is very profound, especially with Ag, Cu, Fe, Ni, Pb and Zn [25].

Low concentrations [i.e. 1–20% (v/v)] of low-molecular-weight organic substances, including ethanol, formic acid and acetic acid, in electrolyte solutions are beneficial for the response achieved for Hg in ELCAD [35]. Accordingly, the presence of 1% (v/v) or 5% (v/v) of formic acid in 0.1 mol/L or 0.2 mol/L HNO_3 electrolyte solutions produced three-fold enhancement of the response for Hg, compared to conditions without addition of the organic acid. The addition of acetic acid to 0.1 mol/L and 0.2 mol/L HNO_3 electrolyte solutions at the level of 5% (v/v) and 10% (v/v) even results in a four-fold improvement in the response for Hg [35]. This signal enhancement is supposed to be due to changes in the boiling point and the surface tension of electrolyte solutions, but it is also probable that H and CO radicals originating from these low-molecular-weight organic acids reduce Hg(II) ions into Hg(0) vapors [47]. However, we also note an extreme sputtering and reduction process of Hg ions in a bulk solution cathode ELCAD system coupled to an ICP-OES instrument [45]. Without any additional substance added to a solution, a 17-fold increase in the signal for Hg, compared to that obtained with PN, is higher than for other elements present in the solution (Al, B, Ba, Ca, Cd, Cr, Cu, Mg, Pb, Zn).

Interestingly, the analytical response is species-dependent. Accordingly, polyatomic anions of Mn and Cr at high oxidation states (MnO_4^-, $Cr_2O_7^{2-}$) produce greater signals than lower oxidation-state atomic cations of these metals at the same concentrations (Mn^{2+}, Cr^{3+}), possibly due to easier migration of these first ions [17]. With Hg, the response can be achieved from not only inorganic species [simple Hg(II) ions] but also organic species of elements, but signals for the latter species are small (i.e. two-fold and four-fold smaller for methyl and thiomersal Hg, respectively) [34].

6. Analytical characteristics

The radiation emitted by dc-APGD generated in contact with electrolyte solutions in different discharge devices is commonly measured in the spectral range 200–800 nm, 185–650 nm [32], or 165–500 nm [33–35], using monochromators equipped with photomultiplier tubes or charge-coupled device (CCD) cameras (as separate instruments or as parts of ICP-OES) [8–13,15–18,20–23,26–38,39,44,46] or polychromators [43]. The strongest line spectra of atoms are observed for the near-cathode region (i.e. NG) [8,9,31,37]. Background intensities in this region are low, so this part of the discharge is analytically the most useful, since signal-to-noise ratios for different elements are the best [31].

Excitation conditions occurring in ELCADs or LS-APGDs, where the analyzed sample solution is one part of the electrode system, result in sputtering the surface of solution cathodes and exciting atoms of elements dissolved in electrolyte solutions being analyzed [8,39]. Because the degree of the ionization is 4–5 times lower than in ICP [29,36] and usually spans the range 10–20%, basic atomic emission lines of different elements are mostly excited [29]. A complete list of analytical atomic and ionic emission lines identified in spectra of different systems of dc-APGD generated in contact with liquid cathodes is given in Table 2. It can be seen that resonant atomic lines of relatively low excitation energies predominate in emission spectra [10,20,39]. Ionic emission lines of Ca, Cu and Mg can also be excited and are identified, but these are marginal [8,9,29,36,38,43,46]. When LS-APGD is used as the ion source,

Table 2. Atomic (I) and ionic (II) emission lines of elements identified in spectra of various direct-current, atmospheric-pressure, glow discharge (dc-APGD) systems generated in contact with flowing electrolyte solutions

Ag	Ag I 338.3 nm [18,21,23,43,44,52[a]]
Al	Al I 396.2 nm [16]
Au	Au I 242.8 nm [21]
Ba	Ba II 493.4 nm [52[a]]
Ca	Ca I 422.7 nm [8,9,15–17,20,21,31–33,37,39], Ca II 393.4 nm [9,37,38,52[a]]
Cd	Cd I 228.8 nm [9,11,16,17,20–23,31,33,38,15[b],51[c],54[d]]
Co	Co I 345.3 nm [31]
Cr	Cr I 357.8 nm [16,31,54[d]], Cr I 425.4 nm [10]
Cs	Cs I 852.1 nm [21,52[a]]
Cu	Cu II 224.7 nm [10], Cu II 229.4 nm [10], Cu I 324.8 nm [8–11,15 18,20–23,31,32,39,44,46,8[b],9[b],16[b],49[e],54[d]], Cu I 327.4 nm [8–10,15–17,33,43,46,8[b],9[b],16[b],50[e],54[d]], Cu I 510.5 nm [8–10,16,31,50[e]], Cu I 465.1 nm [50[b]], Cu I 470.4 nm [50[e]], Cu I 515.3 nm [10,31,50[e]], Cu I 521.8 nm [10,50[e]]
Fe	Fe I 248.3 nm [10,26,32,33], Fe I 373.3 nm [15], Fe I 495.8 nm [32]
Hg	Hg 253.7 nm [18,21,23,27,28,33–35,46], Hg I 365.0 nm [16]
K	K I 766.5 nm [8,9,15,16,20,21,23,37,52[a],54[d]], K I 769.9 nm [8,9,15,16,21,23,37,51[c],54[d]]
Li	Li I 670.8 nm [18,20,21,23,52[a]]
Mg	Mg I 285.2 nm [8,9,15,16,18,20,21,23,27,29,36–38,46,8[b],9[b],15[b],16[b]], Mg II 279.6 nm [8,9,29,36–38], Mg II 280.3 nm [8,9,36,37,43,46], Mg I 518.4 nm [52[a]]
Mn	Mn I 279.5 nm [9,17,18,20,21], Mn I 280.1 nm [9], Mn I 403.1 nm [10,15,16]
Mo	Mo I 344.7 nm [46]
Na	Na I 589.0 and 589.6 nm [8,9,15–18,20,21,23,26–28,31,37–39,44,49[e],51[c],54[d]]
Ni	Ni I 341.5 nm [9,11,21,22,31,43,10[b]]
Pb	Pb I 217.0 nm [16,16[b]], Pb I 368.5 nm [15–17,21,51[c]], Pb I 405.8 nm [9–11,15,16,18,22,23,26,27,31,33,38,54[d]]
Pd	Pd I 340.4 nm [31]
Rb	Rb I 780.0 nm [20], Rb I 794.8 nm [52[a]]
Sc	Sc I 326.9 nm [46]
Sr	Sr II 407.8 nm [52[a],53[a]], Sr II 421.6 nm [52[a],53[a]], Sr I 460.7 nm [21,52[a],53[a]]
Zn	Zn I 213.8 nm [9,11,16,20–22,31–33,38,43,10[b],54[d]],Zn I 481.0 nm [15]

[a] For liquid electrode-dielectric barrier discharge (LE-DBD).
[b] Observed in the second order.
[c] For alternating current electrolyte atmospheric liquid discharge (ac-EALD).
[d] For liquid film-dielectric barrier discharge (LF-DBD).
[e] For a miniaturized electrolyte cathode discharge (ELCAD) system.

discharge devices are coupled to regular mass spectrometers [24,25].

The reproducibility of measured signals (commonly expressed in the form of RSD) in continuous signals obtained with ELCAD or transient signals obtained with LS-APGD is typically in the range 2.0–9.0% [10,16,26], although poorer precisions (10–15%) were also reported [27,28,44]. In ELCAD, this figure of merit, also referred to as short-term precision, is closely related to changes in the size of the discharge and the electrode gap resulting from pulsations of pumps, changes in the temperature of electrolyte solutions or fluctuations in the pressure in discharge cells [9,10,16]. The last of these perturbations is the main reason for the worse analytical performance (i.e. poorer RSD and LOD values) being obtained in earlier ELCAD systems [9,10,16].

As can be seen from Table 3, achievable LODs for different elements are usually in the sub-mg/L range. Surprisingly, LODs obtained with LS-APGD are even higher than those reported for early ELCAD systems [26,27] (see Table 4). Linearity ranges obtained for early ELCAD systems (in mg/L) are relatively short {i.e. from 1 [9] to 2 [32] orders of magnitude}. In LS-APGD, the linearity range also span 2–3 orders of magnitude, although concentrations of upper and lower linearity range limits are higher than those for ELCAD [26–28].

Later modifications of ELCADs, aimed at improving the optical thinness of this source, its stability and the reproducibility of introducing electrolyte solutions and the discharge gap, result in a much better analytical performance [17,18,20,21,33–35]. Mentioned improvements brought LODs within the range 0.001–0.01 mg/L [17,18,20,21,23,33–35], linearity ranges that vary from two to at least four orders of magnitude [17,18,20,23,33–35] and precision in most cases within 0.8–6.5% as RSD [18,20,23,33–35]. Upper linearity limits did not usually exceed 100 mg/L [18,20,23,35], but in some cases they reached even 1000–5000 mg/L [33,34].

7. Analytical applications

Early applications of continuous-flow ELCAD systems reported in analytical OES for the elemental analysis are

Table 3. Limits of detection (LODs) of elements (3σ of the blank criterion) obtained with different electrolyte cathode discharge (ELCAD) systems (in mg/L)

Element	Ref.																
	[9][a]	[10]	[15]	[16]	[17]	[18][c]	[20]	[21]	[22][a,c]	[23]	[32]	[33]	[34]	[35][c]	[37]	[47][d]	[51][e]
Ag						0.002		0.005		0.0003							
Al				0.3													
Au								0.078									
Ca	0.4				0.020		0.09	0.023			0.3	0.017					
Cd	0.1		0.03	0.7	0.010	0.015	0.05	0.009	0.014	0.002		0.005					0.090
Cr		0.2		0.9													
Cs								0.211									
Cu	0.06	0.01	0.01	0.3	0.030	0.024	0.08	0.031	0.022	0.004	0.65	0.011					
Fe		0.02									0.1	0.028					
Hg			0.08	1		0.270		0.349		0.022		0.015	0.015, 0.010[c]	0.002		0.0007, 0.0012[c]	
K	0.2		0.001				0.004	0.013									
Li						0.0002	0.002	0.008		0.00006							
Mg	0.8, 1.5[b]					0.001	0.04	0.019		0.0002							
Mn	0.4, 0.7, 0.8[b]	0.03		0.1		0.011	0.1	0.030									
Na	0.06		0.001		0.0008	0.0004	0.002	0.0008		0.0001					0.003		0.040
Ni	0.4	0.02						0.110	0.034								
Pb	0.8	0.03	0.01	0.3	0.080	0.060		0.082	0.028	0.006		0.045					
Rb							0.04										
Sr								0.049									
Zn	0.1	0.6					0.1	0.042	0.016		0.7	0.003					

[a] 2σ of the blank criterion is used.
[b] Different analytical lines are taken.
[c] A multiple sample loading in the FI mode is applied.
[d] Used as a sample introduction unit for ICP.
[e] Alternating current electrolyte atmospheric liquid discharge (ac-EALD) is used.

Table 4. Limits of detection (LODs) of elements (3σ of the blank criterion) obtained with other atmospheric-pressure, glow discharge (APGD) systems (in mg/L)

Element	Ref.									
	[19][a,b]	[24][a,b,c]	[25][a,b,c]	[26][a,b]	[27][a,b]	[28][a,b]	[43][a,b]	[52][d]	[53][d]	[54][e]
Ag							0.54	0.54		
Ba								6.9		
Ca								1.2		
Cd			0.60							0.038
Cs		0.016	0.05					1.3		
Cu			2.2				0.77			0.075
Fe			0.67	12						
Hg	3				1.9	5			42	
In			0.04							
K								0.020		0.025
Li								0.028		
Mg					1.6		0.93	1.7		
Na	0.2			12	1.3	6			0.064	0.007
Ni			1.0				1.8			
Pb			0.02	14	5.4				40	
Rb								0.60		
Sr								3.5	18	
Zn							0.44			0.079

[a] Liquid sampling-atmospheric pressure glow discharge (LS-APGD) is used.
[b] A multiple sample loading in the FI mode is applied.
[c] LS-APGD is used as the ion source in MS.
[d] Liquid electrode-dielectric barrier discharge (LE-DBD) is used.
[e] Liquid film-dielectric barrier discharge (LF-DBD) is used.

only qualitative and illustrate the usefulness of these unique excitation sources in reference to the radiation intensity of basic discharge components identified (i.e. molecules and atoms) being very promising. Apparently, in the overwhelming majority of works published in 1993–2000 or even later, the use of ELCAD was limited to identifying the presence of Na, K, Ca and Mg ions in tap waters, which are simply used in these systems as electrolyte and/or carrier solutions [8,9,11,13,16,22, 31,38,39]. To demonstrate the suitability of this excitation source for a wider group of metals, tap waters were also spiked with Cu, Pb and other heavy metals {e.g., Cd, Ni, Zn [8,9,13,16,22,38,39]}. Unfortunately, achievable LODs for different elements were usually in the sub-mg/L range (see Table 3), and, for that reason, first trials were not promising for monitoring concentrations of metals, particularly Al, Cd, Cr, Cu, Mn, Pb and Hg, in water samples [16]. In addition, the use of reagents per analysis was also quite high due to the relatively high sample-uptake rates [16].

Later improvements of ELCAD cells meant that this excitation source could provide the quantitative elemental analysis of different liquid samples by OES detection {i.e. tap water [15], drinking water [15], mineral water [20], tea infusion [20], fresh milk [15] or hepatitis-B vaccine samples [34]}. The sample preparation required in the direct analysis of water samples was limited to their acidification [15]. More complex samples (e.g., milk or hepatitis-B vaccines) are appropriately diluted before acidification in order to decrease possible matrix effects [15,34].

The analysis of solid samples is also possible, but requires them to be mineralized prior to measurements in digestion reagents {i.e. mixtures of HNO_3 and H_2O_2 [20,33–35] or HNO_3 and HF [33]} in open-vessel systems [20,35] or closed-vessel systems [33,34]. After the digestion of sample matrices, the resulting sample solutions are evaporated to near dryness and reconstituted with an appropriate acid solution to reach the required pH [20,33–35]. In this way, the following samples are analyzed: certified reference materials of tuna fish {i.e. 350 from the International Atomic Energy Agency (IAEA) [33–35]}, BCR 463 from the Institute for Reference Materials and Measurements (IRMM) [33,34], aquatic plants {i.e. BCR-060 from IRMM [35]}, oyster tissue {i.e. SRM 1566a from the National Institute of Standards and Technology (NIST) [33]}, coal fly ash {i.e. SRM 1633b from NIST [33]}, or tea leaves [20].

Quantification of concentrations of elements is usually based on calibration with external standard solutions [15,20] or using standard additions [33–35]. In the latter case, it is carried out to eliminate any possible matrix effects [33–35]. The analytical performance seems quite promising but there is still much room for improvement. The accuracy of the analysis is in the range 0.6–7% for major and trace elements, while the

precision is in the range 0.6–11% [33–35]. In terms of these figures of merit, simple ELCAD-OES devices can successfully replace other analytical instruments {i.e. ET-AAS and CV-AAS [34], and FAAS and FOES [20]}.

Unfortunately, despite the possibility of analyzing small sample volumes in FI mode, practical application of LS-APGD is limited, since the LODs obtained with this excitation source for different elements are even higher than those reported for early ELCAD systems [26,27] (see Table 4).

8. Conclusions

APGD generated in contact with flowing electrolyte solutions appears to be a very promising excitation source that can be applied successfully to the spectrochemical analysis of liquid samples by OES. The inherent nature of this discharge in addition to atomization and excitation conditions in the near-cathode zone makes its emission characteristics relatively simple and very useful. Small dimensions, low operational costs and low power requirements are other advantages that distinguish it from other bulky excitation sources that are expensive to operate and to maintain. The presence of basic and the most prominent atomic lines of elements in addition to a smaller chance of line coincidences open up the possibility of the portability of the whole measurement system by using smaller spectrometers for observation of the discharge radiation with satisfactory resolution. Achievements coincidently made in recent years in the miniaturization of discharge cells also strengthen this possibility. They result in considerable diminution of the sample-uptake rate and improvement in the analytical performance (e.g., LODs and the reproducibility of the analytical response). More to the point, this development is responsible for reducing complexity and dimensions of the latest electrode-discharge systems.

Certainly, further effort and work are required to improve the analytical characteristics of such dc-APGD systems and to increase the applications in elemental trace analysis by OES and MS. This could be achieved through modifications to the composition and the physicochemical properties of electrolyte solutions serving as liquid cathodes and changes in the design and the materials of electrodes, including capillaries used for delivering electrolyte solutions, anodes and/or counter electrodes. Accordingly, the addition of low-molecular-weight organic compounds can promote the formation of radicals and active species capable of generating volatile species and/or vapors of some selected elements (e.g., As, Cd, and Hg). The presence of surfactants can lower the surface tension of electrolyte solutions and enhance the sputtering efficiency and the transfer rate of elements to the near-cathode zone. A general reduction in dimensions of delivery capillaries used for electrolyte solutions and changes in the geometry and the size of counter electrodes also matter. Such treatment may result in further miniaturization of the electrode system, a decrease in the volume of the discharge and, consequently, increase the power density focused between electrodes of the discharge system and the stability of the discharge operation. Higher current density and reproducibility of the cathode surface can be achieved in these conditions, having a significant impact on increasing the detection power, the repeatability of measurements and the applications of the discharge. We can assume that it would be used as an independent excitation source for OES measurements, but it should also find application as a detector of atomic or molecular components when coupled to high-performance liquid chromatography, or other on-line flow separation or discrete sample-introduction devices.

Acknowledgements

This work was financed by a statutory activity subsidy from the Polish Ministry of Science and Higher Education for the Faculty of Chemistry of Wroclaw University of Technology.

References

[1] R. Foest, M. Schmidt, K. Becker, Int. J. Mass Spectrom. 248 (2006) 87.
[2] J.A.C. Broekaert, V. Siemens, Anal. Bioanal. Chem. 380 (2004) 185.
[3] J. Franzke, K. Kunze, M. Miclea, K. Niemax, J. Anal. At. Spectrom. 18 (2003) 802.
[4] V. Karanassios, Spectrochim. Acta, Part B 59 (2004) 909.
[5] J.A.C. Broekaert, Anal. Bioanal. Chem. 374 (2002) 182.
[6] J. Franzke, M. Miclea, Appl. Spectrosc. 60 (2006) 80A.
[7] M. Miclea, J. Franzke, Plasma Chem. Plasma Process. 27 (2007) 205.
[8] T. Cserfalvi, P. Mezei, P. Apai, J. Phys. D: Appl. Phys. 26 (1993) 2184.
[9] T. Cserfalvi, P. Mezei, J. Anal. At. Spectrom. 9 (1994) 345.
[10] H.J. Kim, J.H. Lee, M.Y. Kim, T. Cserfalvi, P. Mezei, Spectrochim. Acta, Part B 55 (2000) 823.
[11] P. Mezei, T. Cserfalvi, H.J. Kim, M.A. Mottaleb, Analyst (Cambridge UK) 126 (2001) 712.
[12] P. Mezei, T. Cserfalvi, Eur. Phys. J., Appl. Phys. 40 (2007) 89.
[13] P. Mezei, T. Cserfalvi, M. Janossy, K. Szocs, H.J. Kim, J. Phys. D: Appl. Phys. 31 (1998) 2818.
[14] M.R. Webb, G.M. Hieftje, Anal. Chem. 81 (2009) 862.
[15] M.A. Mottaleb, Y.A. Woo, H.J. Kim, Microchem. J. 69 (2001) 219.
[16] Y.S. Park, S.H. Ku, S.H. Hong, H.J. Kim, Spectrochim. Acta, Part B 53 (1998) 1167.
[17] M.R. Webb, F.J. Andrade, G.M. Hieftje, J. Anal. At. Spectrom. 22 (2007) 766.
[18] M.R. Webb, F.J. Andrade, G.M. Hieftje, Anal. Chem. 79 (2007) 7807.
[19] J.L. Venzie, R.K. Marcus, Anal. Bioanal. Chem. 381 (2005) 96.

[20] P. Jamroz, P. Pohl, W. Zyrnicki, J. Anal. At. Spectrom. 27 (2012) 1032.
[21] M.R. Webb, F.J. Andrade, G. Gamez, R. McCrindle, G.M. Hieftje, J. Anal. At. Spectrom. 20 (2005) 1218.
[22] T. Cserfalvi, P. Mezei, J. Anal. At. Spectrom. 18 (2003) 596.
[23] M.R. Webb, F.J. Andrade, G.M. Hieftje, Anal. Chem. 79 (2007) 7899.
[24] R.K. Marcus, C.D. Quarles, C.J. Barinaga, A.J. Carado, D.W. Koppenaal, Anal. Chem. 83 (2011) 2425.
[25] C.D. Quarles, A.J. Carado, C.J. Barinaga, D.W. Koppenaal, R.K. Marcus, Anal. Bioanal. Chem. 402 (2012) 261.
[26] R.K. Marcus, W.C. Davis, Anal. Chem. 73 (2001) 2903.
[27] W.C. Davis, R.K. Marcus, J. Anal. At. Spectrom. 21 (2001) 931.
[28] W.C. Davis, R.K. Marcus, Spectrochim. Acta, Part B 57 (2002) 1473.
[29] M.R. Webb, G.C.Y. Chan, F.J. Andrade, G. Gamez, G.M. Hieftje, J. Anal. At. Spectrom. 21 (2006) 525.
[30] P. Mezei, T. Cserfalvi, J. Phys. D: Appl. Phys. 39 (2006) 2534.
[31] P. Mezei, T. Cserfalvi, L. Csillag, J. Phys. D: Appl. Phys. 38 (2005) 2804.
[32] A. Shaltout, Microchim. Acta 155 (2006) 447.
[33] R. Shekhar, D. Karunasagar, M. Ranjit, J. Arunachalam, Anal. Chem. 81 (2009) 8157.
[34] R. Shekhar, D. Karunasagar, K. Dash, M. Ranjit, J. Anal. At. Spectrom. 25 (2010) 875.
[35] R. Shekhar, Talanta 93 (2012) 32.
[36] P. Jamroz, W. Zyrnicki, Plasma Chem. Plasma Process. 31 (2011) 681.
[37] P. Jamroz, W. Zyrnicki, P. Pohl, Spectrochim. Acta, Part B 73 (2012) 26.
[38] P. Mezei, T. Cserfalvi, M. Janossy, J. Anal. At. Spectrom. 12 (1997) 1203.
[39] T. Cserfalvi, P. Mezei, Fresenius, J. Anal. Chem. 355 (1996) 813.
[40] M.A. Mottaleb, J.S. Yang, H.J. Kim, Appl. Spectrosc. Rev. 37 (2002) 247.
[41] P. Mezei, T. Cserfalvi, Appl. Spectrosc. Rev. 42 (2007) 573.
[42] P. Mezei, T. Cserfalvi, Sensors 12 (2012) 6576.
[43] C.D. Quarles, B.T. Manard, C.Q. Burdette, R.K. Marcus, Microchem. J. (2012). http://dx.doi.org/10.1016/j.microc.2012.01.012.
[44] W.C. Davis, D. Strand, R.K. Marcus, Am. Lab. 4 (2003) 28.
[45] T. Cserfalvi, P. Mezei, J. Anal. At. Spectrom. 20 (2005) 939.
[46] J.L. Venzie, R.K. Marcus, Spectrochim. Acta, Part B 61 (2006) 715.
[47] Z. Zhu, G.C.Y. Chan, S.J. Ray, X. Zhang, G.M. Hieftje, Anal. Chem. 80 (2008) 7043.
[48] G. Jenkins, A. Manz, J. Micromech. Microeng. 12 (2002) N19.
[49] G. Jenkins, J. Franzke, A. Manz, Lab Chip 5 (2005) 711.
[50] M.F. Zorn, C.G. Wilson, Y.B. Gianchandani, M.A. Anderson, Sensor Lett. 2 (2004) 179.
[51] R. Huang, Z. Zhu, H. Zheng, Z. Liu, S. Zhang, S. Hu, J. Anal. At. Spectrom. 26 (2011) 1178.
[52] T. Krahling, S. Muller, C. Meyer, A.K. Stark, J. Franzke, J. Anal. At. Spectrom. 26 (2011) 1974.
[53] S. Tombrink, S. Muller, R. Heming, A. Michels, P. Lampen, J. Franzke, Anal. Bioanal. Chem. 397 (2010) 2917.
[54] Q. He, Z. Zhu, S. Hu, H. Zheng, L. Jin, Anal. Chem. 84 (2012) 4179.
[55] A.V. Khlyustova, A.L. Maksimov, M.S. Khorev, Surf. Eng. Appl. Electrochem. 44 (2008) 370.